

A Real-Time Haze Removal & Mosaicing using Rapid Prototype Hardware



Sai Venu Prathap Katari, K. Kishore Kumar, K Gopi

Abstract: In this paper, a pivotal technique was proposed that reduces the haze and combines the haze free image to increase the Field of View (FoV) in real-time with a rapid prototype hardware device. The Initial focus is to reduce the haze in an image with Dark Channel Prior Technique and the FSD method is utilized to mosaic the haze free images. Low contrast may occur due to the scattering light, air particles or fog in nature which results in a haze image that needs to be reduced and enhance the image for better vicinity. Haze reduction approach depends on entropy and information fidelity. Our Haze free algorithm executes multiple phases such as dark channel prior computation, estimation and refinement of transmission map and restoration of RGB values. The second technique is the mosaic process that improves the field of view of a scene and the phases that execute are corner detection, extraction, geometric computation and blending. Our experimental results have shown better when compared to the other algorithms. The whole process is executed in real-time with a standalone device called Intel compute stick.

Keywords: Haze, Dark Channel Prior, Mosaic, Steerable filters, FAST, Corner detection.

I. INTRODUCTION

Lightning conditions play a pivotal role to capture the details of a scene in real-time. The acquired images have a low dynamic range with more noise that degrades the overall computation of the image processing algorithms or computer vision techniques. To obtain the robust performance on the haze or low contrast images our approach utilizes the low light enhancement or haze reduction algorithms that result in good visibility of an image. The main aim of this paper is to enhance the low light images that are captured in real-time and to construct the mosaic image with a standalone device. Mosaic is a process of combining multiple partial parts of a scene to produce a single mosaic image that has increased FoV of a scene. The FoV of an adult human being is $180^\circ \times 220^\circ$ where 180° indicates the horizontal FoV and 220° indicates the vertical FoV of a scene. The compact camera FoV is $50^\circ \times 30^\circ$, so a single shot of an imaging sensor never provides an FoV of a human being. In this situation, the mosaic plays a pivotal role to improve the FoV of an imaging sensor. Our research was computed in two phases, the initial phase employs with the dehazing technique which is a challenging task in several real-time image processing applications. The haze or low contrast images degrades the performance of the further process.

Revised Manuscript Received on August 30, 2020.

* Correspondence Author

Dr. Sai Venu Prathap K., Associate Professor, Department. of ECE, Sri Venkateswara College of Engineering (SVCE), Tirupati (A.P), India.

K Kishore Kumar, Assistant Professor, Dept. of ECE, Sri Venkateswara College of Engineering (SVCE), (A.P), India.

K Gopi, Assistant Professor, Department. of ECE, SVCE-Tirupati. (A.P), India.

© The Authors. Published by Blue Eyes Intelligence Engineering and Sciences Publication (BEIESP). This is an open access article under the CC BY-NC-ND license (<http://creativecommons.org/licenses/by-nc-nd/4.0/>)

In cloudy climatic conditions, the satellite images may consist of low contrast or haze which need to be enhanced for better information or details from the images. During winter and rainy seasons, the satellite images may consist of haze or poor dynamic range or low contrast. This image needs to be enhanced to obtain some sort of detail. In hill stations, forest areas and remote sensing areas the human beings have more difficult to acquire the real-time images with high dynamic range. In this scenario, the standalone devices that can attach with the UAV are utilized to capture the remote sensing areas in real-time at a low altitude. If this acquired image consists of haze or low contrast, our system enhances the images and performs the mosaic process to produce the mosaic with more details and FoV. There are several haze removal techniques, each algorithm has a specific application. The haze reducing methods [1] are broadly classified into three categories such as restoration techniques, fusion techniques and enhancement techniques as depicted in fig.1. In 2008 Tan [2] introduced a modern haze removal method depending on the two observations such as air light and enhancement visibility. This technique enhances the local contrast depending on the Markov Random Field, but the shortcoming of this approach was it generates over saturated images.

In 2008, Fatal [3] introduced an algorithm that reduces the haze effect from the colour images. This algorithm depends on the Independent Component Analysis. This technique takes more computation time and strictly confined only for color images but not applicable for grayscale pictures. As the haze dense increases, the performance of this technique decreases.

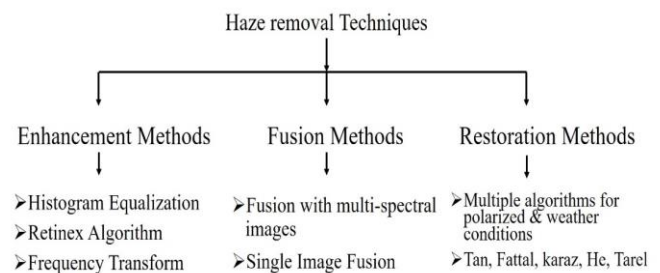


Fig. 1. Classification of Haze Removal Techniques

In 2015 Huimin [4] et al. proposed the optimized dehazing algorithm that computes the atmospheric light effectively and minimizes the fog by the semi globally adaptive filter technique. This algorithm shows good results for the darker environmental images. In 2016 livington et al.,[5] proposed a dehazing method that depends on the visibility of the restoration. The enhancement of the haze or low contrast images has multiple applications in real-time applications such as monitoring the remote sensing areas, natural disasters, R & B department,



CCTV footage surveillance, driver guiding systems, underwater imaging and so on. The proposed work employs a dark channel prior to technique [DCP]. This method increases the Low Dynamic Range (LDR) into the High Dynamic Range (HDR)[6]. The second phase is to produce the mosaic image, that computes the corner detection, extraction, matching, geometric computation, warp and blend methods. The detected corners should be invariant to illumination, angle, scaling and orientation. The FREAK binary descriptor is utilized to extract the corner points. Geometric computation maps the feature points of two distinct images of the same scene.

II. WORKFLOW OF PROPOSED SYSTEM

A. Distinct Weather Conditions

Image acquisition in distinct weather conditions such as sunny and hazy weather conditions is depicted in fig.2. The sun is the source of the light, scene or objects that observes some sort of illuminated light from the sun and reflects some amount of light. Equation.1 depicts the total light energy of the captured image $F(x,y)$ which is a product of the illumination energy $I(x,y)$ and reflectance energy.

$$F(x,y) = I(x,y) \cdot R(x,y) \quad (1)$$

The depth of the haze in the image is computed. It depends on the distance between the scene and the camera as illustrated in fig.2. The HDR of the images depends on the atmospheric scattering light, quality of the camera lens, climatic conditions and so on.

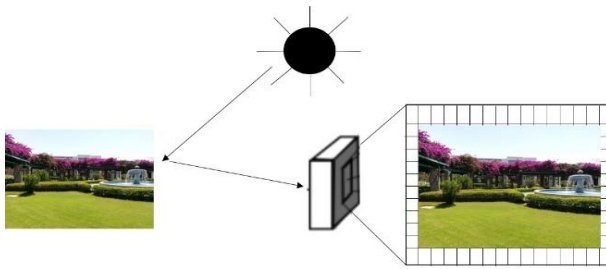


Fig.2.(a) Image Acquisition in sunny weather

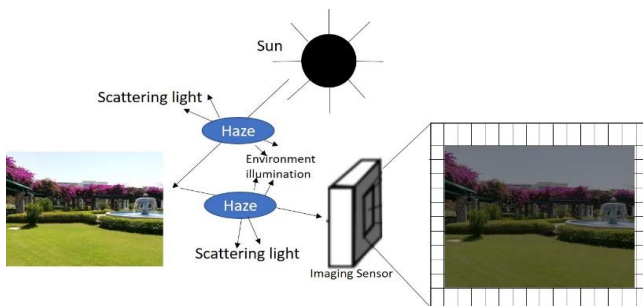


Fig. 2.(b) Image Acquisition in hazy weather & Scattering of Atmospheric Light

Fig.2(a) depicts the haze free image, in sunny condition, the source illuminate's energy that falls on the scene and the scene objects observes little energy and reflects more energy. The imaging sensor gathers the reflected energy from the scene objects and emphasizes the energy on the imaging plane. Usually in sunny weather outdoor pictures consists of vivid colours. Fig.2(b) depicts the image captured in hazy weather under two parameters such as air light and attenuation [7].

The hazy image consists of low contrast due to the direct attenuation occurred by the decrease in reflected energy.

In the atmospheric scattering technique [8] represented by equation 3, the direct attenuation is illustrated by the term $R(x)t_m(x)$. It denotes that in the image the intensity of the pixel degrades by the multiplicative approach.

$$H(x) = R(x)t_m(x) + A_L(1 - t_m(x)) \quad (3)$$

where $t_m(x) = e^{-\beta d(x)}$

x = Pixel position in an image, H =hazy image, R = haze free image scene radiance, t_m = transmission medium, d = depth of the scene, A_L = atmospheric light, β = coefficient of the scattering light.



Fig. 3. Sample of image dehazing using the proposed algorithm

The air-light [9] obtained by the environment scattering illumination decreases the saturation and increases the brightness. In equation 3 the term $A_L(1 - t_m(x))$ shows the air light effect. Therefore, hazy pixels of an image is obtained due to less saturation and more brightness as shown in equation 3. Haze in the image usually degrades the visibility range and leads to a poor or incorrect result when computed by the image processing algorithms. Haze free images have more information and lead to a robust result when they are computed by the computer vision algorithms and they are as shown in fig.3.

The fig.4 Depicts the workflow of the proposed system that includes the haze removal process and mosaicing technique and explained with the following steps

Step 1: The scene is captured with the digital camera in real-time.

Step 2: Haze of the input image is removed by the Dark Channel Prior Technique.

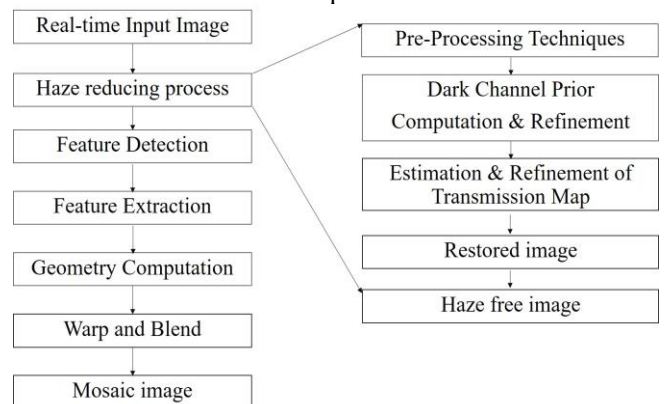


Fig. 4. Block Diagram of Haze free process and mosaicing technique.

- Step 3: Dynamic orientation is selected from the steerable filter bank to generate filter image.
- Step 4: Invariant corners are detected by the FAST method
- Step 5: Features are extracted by using the binary FREAK descriptor.
- Step 6: Geometric transformation is computed for mapping the corner points done on the target
- Step 7: Geometric distortions in an image can be corrected with the warping.
- Step 8: Image blending minimizes the seams in the mosaic image.

B. Intel Compute Stick

This is a standalone pen drive size device that consists of inbuilt licensed windows OS [10]. It transforms any display into a computer and extended memory of the flash drive. It consists of a quad-core Intel® Atom™ processor that gives you balanced performance for work or play and it is as shown in fig. 5.

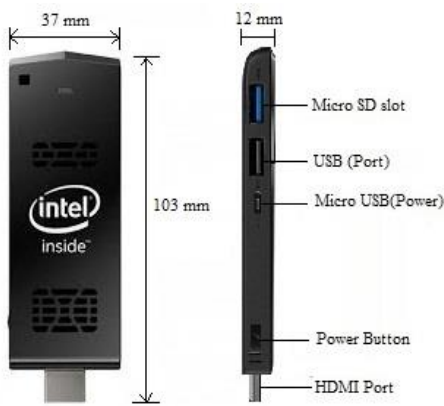


Fig. 5. Block Diagram of Haze free process and mosaicing technique.

III. HAZE REDUCTION & FEATURE DETECTION METHODS

A. Dark Channel Prior

In 1976 McCartney [11] proposed an atmospheric scattering algorithm based on this technique hazy image formation can be explained clearly. This technique is utilized ideally in many image processing and computer vision applications. later Simhan [12,13] and Nayar enhanced this technique and expressed as in equation 3

In 2009, Tang et al. proposed a new dark channel prior (DCP) technique. This model is depending on the low intensity pixels which are popularly known as “dark pixels” excluding in the sky regions [14]. Depending on the research approach the dark channel is defined as

$$D_c = \min_{y \in \Omega(x)} (\min_{c \in \{R,G,B\}} I^c(y)) \quad (4)$$

I^c = intensity of color channel
 $\Omega(x)$ = localpatch centered

Three parameters play an essential role in the formation of the low intensities among the dark channel such as

1. Dark substances
2. Colourful exteriors
3. Shadows

Depending on the above features the dark channel pixel value is estimated as

$$D_c \approx 0$$

This estimation to 0 of the dark channel pixel value is recognized as DCP. Computation of the transmission map leads to a few issues such as wrong textures and artifacts. The block min approach reduces the dark channel resolution and forms a blurry transmission map. It can be reduced by the further sharpening approach of a transmission map [15].

B. FAST-Steerable Detector (FSD)

The proposed FSD algorithm is robust and derived from the FAST detector and steerable filters [16]. The FAST stands for Features from Accelerated Segment Test. In 2006 Edward et al., introduced the FAST algorithm [17]. The performance of the FSD is calculated in terms of detected corners, matched corners, computation time and accuracy. The fig.6 depicts the FSD method for corner detection. The haze free image is given as an input to the steerable filter bank. Dynamically the filter bank selects a suitable angle at which the number of strong corners is detected. The FAST corner detector computes the corners in the haze free steered image at a certain angle. The detected corners should be invariant to the illumination, angle and scale. Finally, the robust corners are detected by the FSD technique. The performance of the FSD method has promising results in improving the CCN, accuracy and matching score by reducing the false corner points.

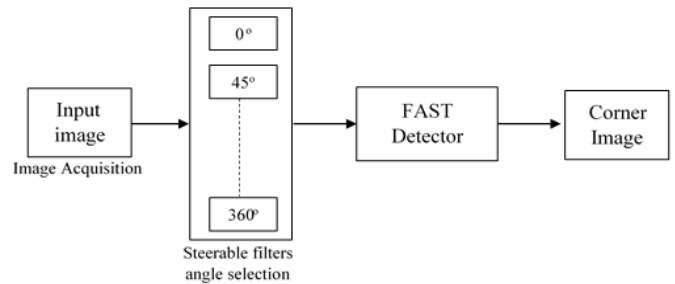


Fig. 6. Proposed FSD corner detector

Corners have more repeatability and good local information. FAST detects corners by taking 16 surrounding pixels to the center pixel. It inspects each pixel by a segmented circle of equal radius from the center pixel as illustrated in the below fig. 7.

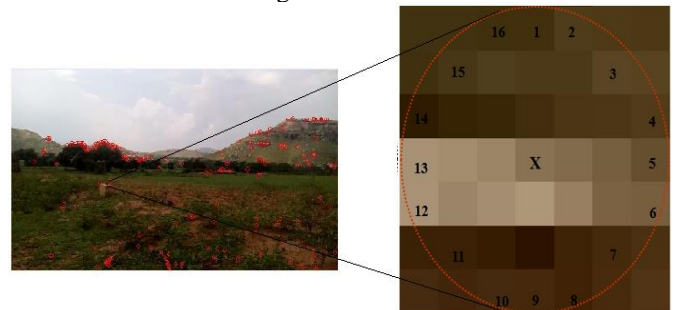


Fig. 7. Sixteen(16) neighbourhood circle segment test of a center pixel ‘X’

C. FREAK Feature Descriptor

FREAK is one of the best binary descriptors. It extracts the data around the detectors. In 2012, Ortiz et al., inspired by the human eye and proposed the FREAK descriptor [18]. Human vision employs DoG to drags the data from the images. Various photoreceptors influence the ganglion cells. FREAK imitates the human visual framework particularly the retina, it has a retinal round examining grid as illustrated in fig.8.

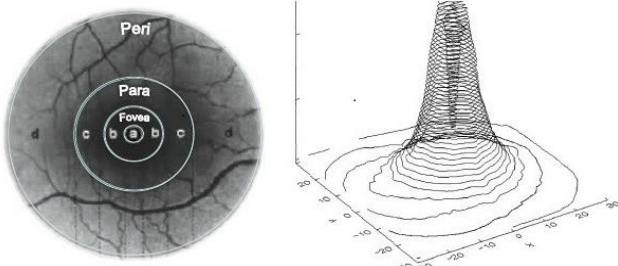


Fig. 8.a) Area of a Retina b) Density of Ganglion cells

IV. APPENDIX

The number of pixels having less intensity value i.e., less than 10 is considered as the number of dark pixels in the processed image P . As the number of dark pixels increases the image quality decreases.

$$No. of\ darkpixels = \sum_{i=0}^{M-1} \sum_{j=0}^{N-1} P(x, y)$$

Avg. Gradient is shown in below equation

$Avg.Gradient = \sqrt{G_x^2 + G_y^2}$ here G_y and G_x is the gradients in y and x directions respectively [19]

Image contrast is illustrated in the below equation

$$I_c = \frac{(Max_L - Min_L)}{(Max_L + Min_L)}$$

Max_L and Min_L are the maximum and minimum luminance values of a haze free resultant image

PSNR between the processed and original images is given by

$$PSNR = 10 \log \left(\frac{(2^n - 1)^2}{MSE} \right)$$

Where MSE is the Mean Square Error

$$MSE = \frac{\sum_{x=0}^{M-1} \sum_{y=0}^{N-1} (P(x, y) - I(x, y))^2}{MN}$$

Peak mean square error is given by

$$PMSE = \frac{\sum_{x=0}^{M-1} \sum_{y=0}^{N-1} (P(x, y) - I(x, y))^2}{MN \sum_{x=0}^{M-1} \sum_{y=0}^{N-1} (\max(I(x, y)))^2}$$

here M and N are the image height and width respectively. As the PMSE increases the image quality decreases.

True corners is the ratio of the matched corners to the average of the ground truth corners and particular algorithmic corners

$$C_{True} = \frac{MatchedCorners(C_m)}{Avg(C_g, C_a)}$$

Here C_g is the no. of ground truth corners and C_a no. of corners that are detected by a specific algorithm. Ground truth corners are majority human judgment corners Accuracy is computed by the no. of matched corners, ground truth corners and no. of corners detected by a specific algorithm and is given by

$$Accuracy = 100 * \left(\frac{\frac{C_m}{C_a} + \frac{C_m}{C_g}}{2} \right)$$

V. EXPERIMENTAL RESULT

The performance of the haze removal methods is evaluated with several parameters. The DCP has the best performance in terms of image contrast, Avg. gradient, computation time and repeatability as illustrated in Table 1.

Table 1: Comparison of DCP and Luminance Component methods with various parameters for sample dehaze image shown in fig.3

Parameters	Dark Channel Priori	Based on Luminance Component
Image Contrast	0.89	0.78
Avg. Gradient	1.24	0.86
No. of Dark Pixels	1787	123
Computation time (m sec)	1454	1865
Peak signal to noise ratio(dB)	22.58	21.56
Repeatability (%)	0.21	0.11
Peak Mean Square Error	0.28	0.36

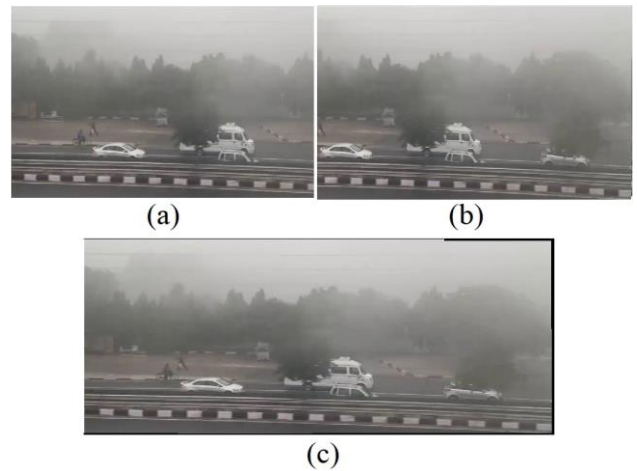


Fig. 9.a)hazy image-1 b)hazy image-2 c) hazy mosaic image

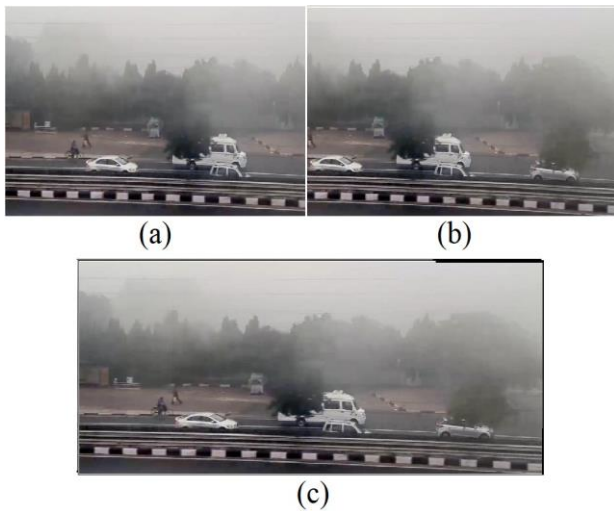


Fig. 10. a)Dehazy image-1 b)Dehazy image-2 c) Dehazy mosaic image

Fig.9(a) and (b) depicts the two hazy images and fig.9(c) shows the hazy mosaic image with poor visibility information. The haze in the captured images is reduced and computed the mosaic image as shown in fig.10. it has two enhanced dehazed images as input and the resultant mosaic image is shown in fig.10(c). The dehaze mosaic image has improved FoV and more visibility information compared to the haze mosaic image.

Table 2: Computation of various parameters for Hazy images

Parameters	Input-1	Input-2	Mosaic image
Image Contrast	0.69	0.71	0.71
Avg. Gradient	1.24	1.31	1.28
PSNR(dB)	18.58	17.25	18.04
PMSE	0.38	0.36	0.35

A comparison of hazy images and dehaze images is shown in Table 2 and Table 3. Dehaze images have better image contrast, Avg, gradient, PSNR and PMSE compared to the hazy images. The Table 4 depicts the computation of the ground truth corners (C_g), detected corners by a specific algorithm (C_a), matched corners between ground truth and detected corners(C_m), true corners, accuracy and computation of the various corner detectors for the synthetic image shown in the figures (a).

Table 3: Computation of parameters for Dehaze images

Parameters	Input-1	Input-2	Mosaic image
Image Contrast	0.74	0.77	0.76
Avg. Gradient	1.56	1.85	1.82
PSNR(dB)	22.58	21.49	22.12
PMSE	0.28	0.22	0.26

Though the Harris algorithm has quick computation time, it has poor Accuracy, True corners and Matched corners than the FSD. The proposed FSD has a good matching score and detected more true corners than the other algorithms. The computation time of FSD is 1.39 times faster than the KLT and 1.65 times faster than the SUSAN algorithm.

Table 4: Comparison of various corner detectors with True corners, Accuracy and Computation time

Algorithm	Ground truth corners (C_g)	Detected corners (C_a)	Matched corners (C_m)	True corners	Accuracy	Computation time(sec)
Harris	35	47	31	75.60	77.26	0.89
SUSAN	35	58	33	70.96	75.59	1.52
KLT	35	62	32	65.97	73.94	1.28
Proposed FSD	35	36	31	88.06	87.34	0.92

VI. CONCLUSION

Haze free methods and mosaicing methods play a pivotal role in several real-time outdoor scenarios. Multiple parameters are computed by the popular two methods among them Dark channel prior method has better PSNR, computation time, repeatability, Peak Mean Square Error and image contrast outcomes than the luminance component algorithm. For mosaicing, four feature detector algorithms are compared in which the proposed FSD algorithm has better true corners, accuracy and matched corners than the Harris, KLT and SUSAN algorithms. The computation time of FSD is 1.39 times faster than the KLT and 1.65 times faster than the SUSAN algorithm.

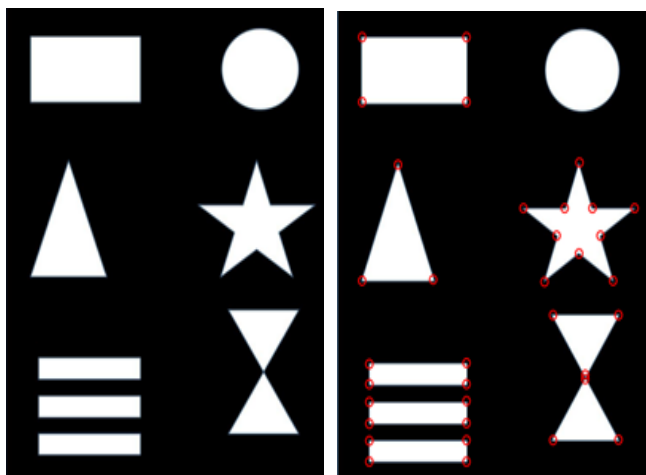


Fig. 11. a)Synthetic image b) Ground Truth corners of a synthetic image

A Real-Time Haze Removal & Mosaicing using Rapid Prototype Hardware

FSD has enough computation time for real-time applications and it is 1.39 times faster than the KLT and 1.65 times faster than the SUSAN algorithm and almost all equal to the Harris algorithm. Finally, this paper proposes a hybrid method that has combined the two techniques such as haze free method and mosaicing methods that has the best experimental promising outcomes than the other algorithms

REFERENCES

1. Wencheng W., Member, Xiaohui Y., "Recent Advances in Image Dehazing" IEEE/CAA Journal of Automatic Sinica, Vol. 4, No. 3, July 2017.
2. R. T. Tan, "Visibility in bad weather from a single image," in Proc. IEEE Conference on Computer Vision and Pattern Recognition (CVPR), 2008, pp. 1-8.
3. R. Fattal, "Single image dehazing," ACM Transactions on Graphics (TOG), vol. 27, no. 3, pp. 72, 2008.
4. Lu, Huimin & Li, Yujie & Nakashima, Shota & Serikawa, Seiichi. Single Image Dehazing through Improved Atmospheric Light Estimation. Multimedia Tools and Applications. Vol. 7, Issue 1, May 2015. V10.1007/s11042-015-2977-7.
5. Merlin L., Agnel L. "Haze Image Enhancement Using Visibility Restoration Technique" IJLTET, Vol. 7, Issue 1, May 2016.
6. R. Gonzalez and E. Richard, "Woods, digital image processing," ed: Prentice Hall Press, ISBN 0-201-18075-8, 2002.
7. S. G. Narasimhan and S. K. Nayar. "Contrast restoration of weather degraded images," *IEEE Trans. Pattern Analysis and Machine Intelligence (TPAMI)*, vol. 25, no.6, pp. 713-724, 2003.
8. E. J. McCartney, Optics of the Atmosphere: Scattering by Molecules and Particles. New York, USA: John Wiley and Sons, Inc., 1976, pp. 1;42.
9. M. Pedone and J. Heikkila, "Robust airlight estimation for haze removal from a single image," in Proc. 2011 IEEE Computer Society Conf. Computer Vision and Pattern Recognition Workshops, Colorado Springs, CO, USA, 2011, pp. 90;96.
10. K.S.V. Prathap, S.A.K.Jilani and P. R. Reddy "A Real-time Image Mosaic Performance Measurements" International Journal of Pure and Applied Mathematics, Vol. 118 No. 18 2018, 3699-3706
11. E. J. McCartney, "Optics of the atmosphere: scattering by molecules and particles," New York, John Wiley and Sons, Inc. 1976.
12. S. G. Narasimhan and S. K. Nayar. "Vision and the atmosphere," *International Journal of Computer Vision (IJCV)*, vol. 48, no. 3, pp. 233-254, 2002.
13. S. G. Narasimhan and S. K. Nayar, "Removing weather effects from monochrome images," in Proc. IEEE Conference on Computer Vision and Pattern Recognition (CVPR), 2001.
14. K He, J Sun, X Tang, Proceedings of IEEE Computer Society Conference on Computer Vision and Pattern Recognition (CVPR, Miami, 2009), pp. 1956-1963
15. K He, J Sun, X Tang, Single image haze removal using dark channel prior. *IEEE Trans. Pattern Anal. Mach. Intell.* 33(12), 2341-2353 (2010)
16. K.S.V. Prathap, S.A.K.Jilani and P. R. Reddy "A Real-time Image Mosaicing using Single Board Computer" *Journal of Engineering and Applied Sciences* Vol. 14, Issue 10, 3150-3157, 2019.
17. Edward Rosten, Reid Porter, and Tom Drummond. Faster and Better: "A Machine Learning Approach to Corner Detection". *IEEE Transactions on Pattern Analysis and Machine Intelligence*, Vol.32, No.1, January-2010.
18. Alahi, Alexandre, Raphael Ortiz, and Pierre Vandergheynst. "Freak: Fast retina keypoint." *Computer Vision and Pattern Recognition (CVPR)*, IEEE Conference on. IEEE, 2012.
19. V. Vora, A. Suthar, Y. Makwana, and S. Davda, "Analysis of compressed image quality assessments" *IJAEA*, Jan. 2010



K Kishore Kumar, Assistant Professor, Dept. of ECE, Sri Venkateswara College of Engineering (SVCE)-Tirupati. Graduated from Anna University Affiliated College in 2008, PG in Embedded Systems in 2016. Research Area is Digital Image Processing and Embedded Systems



K Gopi, Assistant Professor, Dept. of ECE, SVCE-Tirupati. He Graduated from JNTUH Affiliated college in 2010, PG from MITS in DECS in 2012. Research Area is Embedded Systems and Signal Processing

AUTHORS PROFILE



Dr. Sai Venu Prathap K., Associate Professor, Dept. of ECE, Sri Venkateswara College of Engineering (SVCE), Tirupati. Graduated from JNTUA affiliated college in 2009, PG in VLSI Design from SRM University in 2011 and has received a doctorate in 2019 from JNTUA. Research Area is Image Processing and Embedded Systems.